

Reinforced Concrete Model for Low Reinforcement Ratios

P.C.J. Hoogenboom, A. Scarpas

Department of Civil Engineering and Geosciences, Delft University of Technology
Delft, The Netherlands

W. Voskamp

Voskamp Internet Services
Delft, The Netherlands

ABSTRACT

A commonly used material model for reinforced concrete walls is the modified compression field theory. In this paper it is shown that this model predicts a too high strength for low reinforcement ratios. A modification is proposed to improve the material model. The accuracy of the solution is shown and size effects are demonstrated.

KEY WORDS: Modified Compression Field Theory, Reinforced Concrete, Low Reinforcement Ratios, Size Effect, Plane Stress, Material Behaviour, Crack Width, Material Stresses, Ultimate Limit State

INTRODUCTION

The ultimate load of concrete elements without reinforcement strongly depends on the tensile strength of the material. Typically, the tensile strength of concrete has a small average and a large standard deviation. Moreover, concrete fracture shows a strong size effect because large members fail at smaller stresses than small members. In reinforced concrete these disadvantages are partly compensated by the properties of the reinforcing steel. However, for low reinforcement ratios the tensile properties of concrete dominate the member behaviour.

Despite the poor properties, practitioners want to apply reinforced concrete with low reinforcement ratios in situations where they feel that reinforcement is almost redundant. Also, codes of practice allow low reinforcement ratios in some situations. In the context of performance-based design the low reinforcement ratios are not prohibited, instead the structural consequences are shown.

In the following Section the mathematical formulation of the MCFT is explained. In the third and fourth Section the equilibrium check of the MCFT and the formulation of crack widths are presented which are particularly important for low reinforcement ratios and size effect. In the fifth Sections the computational algorithm is explained. In the sixth Section size effects in the MCFT are investigated. In the seventh Section the MCFT is applied to predict the behaviour of panels with low reinforcement ratios. An improvement to the MCFT is proposed and it is shown that the improved material model provides a better

agreement with experimental results.

MATERIAL MODEL

The modified compression field theory (MCFT) is a constitutive model for reinforced concrete subjected to plane stress static loading. In this paper the theory is formulated such that it can correctly handle tension and cracking in two directions, both positive and negative shear loading.

$$\begin{array}{c} \left[\begin{array}{c} \varepsilon_{xx} \\ \varepsilon_{yy} \\ \gamma_{xy} \end{array} \right] \xRightarrow{(1)} \left[\begin{array}{c} \varepsilon_{xx} \\ \varepsilon_{yy} \end{array} \right] \xRightarrow{(2)} \left[\begin{array}{c} f_{sx} \\ f_{sy} \end{array} \right] \xRightarrow{(4)} \left[\begin{array}{c} \sigma_{xx} \\ \sigma_{yy} \\ \sigma_{xy} \end{array} \right] \\ \left[\begin{array}{c} \varepsilon_{xx} \\ \varepsilon_{yy} \\ \gamma_{xy} \end{array} \right] \xRightarrow{(1)} \left[\begin{array}{c} \varepsilon_1 \\ \varepsilon_2 \\ \theta \end{array} \right] \xRightarrow{(3)} \left[\begin{array}{c} f_{c1} \\ f_{c2} \\ \theta \end{array} \right] \end{array}$$

Figure 1. Structure of the MCFT

Input of the MCFT consists of the strains ε_{xx} , ε_{yy} and γ_{xy} (Fig 1.). The elementary length over which the strains are computed is approximately equal to the crack distance (Fig. 2). As a consequence the local deformation in the cracks is evenly distributed over the surface. In step 1 the strains are used to compute the principle strains ε_1 and ε_2 and the principle strain direction θ . The equations follow from Mohr's Circle.

$$\begin{aligned} \varepsilon_1 &= \frac{1}{2}(\varepsilon_{xx} + \varepsilon_{yy} + r) \\ \varepsilon_2 &= \frac{1}{2}(\varepsilon_{xx} + \varepsilon_{yy} - r) \\ \cos 2\theta &= \frac{\varepsilon_{yy} - \varepsilon_{xx}}{r} \\ \sin 2\theta &= \frac{\gamma_{xy}}{r} \end{aligned} \quad r = \sqrt{(\varepsilon_{xx} - \varepsilon_{yy})^2 + \gamma_{xy}^2} \quad (1)$$

The reinforcing bars are directed in the x and y directions. In step 2 the stresses in the reinforcement are computed (Fig. 3). These stresses can

be interpreted as an average over the length of the bars. Hardening, breaking and buckling of the bars are not modelled.

$$f_s(\varepsilon) = \begin{cases} f_y & \text{if } \varepsilon > \varepsilon_y \\ E_s \varepsilon & \text{if } -\varepsilon_y \leq \varepsilon \leq \varepsilon_y \\ -f_y & \text{if } \varepsilon < -\varepsilon_y \end{cases} \quad (2)$$

where $\varepsilon_y = \frac{f_y}{E_s}$, E_s is the steel Yong's modulus and f_y is the steel yield stress.

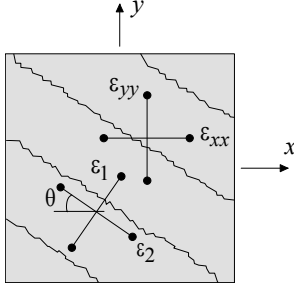


Figure 2. Strains in Reinforced Concrete

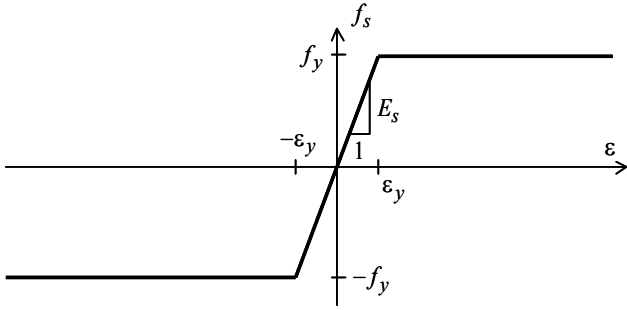


Figure 3. Stress-strain diagram of reinforcing steel in the MCFT

In step 3 the principle stresses in the concrete are computed (Fig. 4.). These equations have been derived from experiments on 30 reinforced concrete panels (Vecchio 1986). The behaviour of the compressed concrete is modelled by a parabola. The compressive strength $f_{c\max}$ is reduced by the strain ε_t in the lateral direction. The behaviour of the tensioned concrete is linear until it cracks. The concrete between the cracks is tensioned because it is extended by the enclosed reinforcement (tension-stiffening). Therefore also after cracking an average concrete stress occurs. The principle stress direction equals the principle strain direction (co-axiality).

$$f_c(\varepsilon, \varepsilon_t) = \begin{cases} 0 & \text{if } \varepsilon < 2\varepsilon'_c \\ f_{c\max} \left(2\frac{\varepsilon}{\varepsilon'_c} - \left(\frac{\varepsilon}{\varepsilon'_c}\right)^2 \right) & \text{if } 2\varepsilon'_c \leq \varepsilon \leq 0 \\ \frac{f_{cr}}{\varepsilon_{cr}} \varepsilon & \text{if } 0 \leq \varepsilon \leq \varepsilon_{cr} \\ \frac{f_{cr}}{1 + \sqrt{200\varepsilon}} & \text{if } \varepsilon > \varepsilon_{cr} \end{cases} \quad (3)$$

$$f_{c\max} = \frac{f'_c}{0.8 - 170\varepsilon_t} \leq f'_c \quad \varepsilon'_c = 2\frac{f'_c}{E_c} \quad \varepsilon_{cr} = \frac{f_{cr}}{E_c} \quad (4)$$

where E_c is the concrete Yong's modulus, f'_c is the compressive strength (negative value), f_{cr} is the tensile strength and ε_t is the strain in the lateral direction.

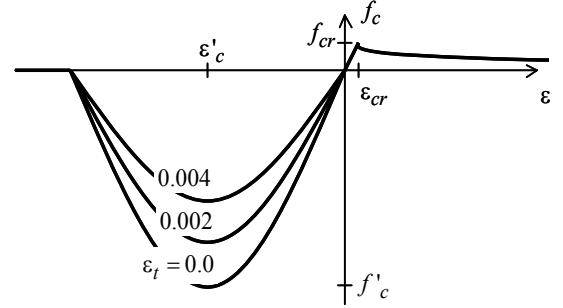


Figure 4. Stress-strain diagram of concrete in de MCFT

In step 4, equilibrium in the cracks is checked. When necessary the average concrete stress $|f_{c1}|$ is reduced. This is explained in the next section. Subsequently, the concrete stresses are rotated to the x - y reference frame using Mohr's circle.

$$\begin{aligned} f_{cx} &= a - b \cos 2\theta & a &= \frac{1}{2}(f_{c1} + f_{c2}) \\ f_{cy} &= a + b \cos 2\theta & b &= \frac{1}{2}(f_{c1} - f_{c2}) \\ v_c &= b \sin^2 \theta \end{aligned} \quad (5)$$

Finally the stresses in the concrete and steel are averaged.

$$\begin{aligned} \sigma_{xx} &= \rho_x f_{sx} + (1 - \rho_x) f_{cx} \\ \sigma_{yy} &= \rho_y f_{sy} + (1 - \rho_y) f_{cy} \\ \sigma_{xy} &= v_c \end{aligned} \quad (6)$$

EQUILIBRIUM IN A CRACK

An essential part of the modified compression field theory (MCFT) is an equilibrium check of the stresses in the cracks. When the computed stresses cannot be carried through the cracks the concrete stress f_{c1} is reduced. Unfortunately, the MCFT is not clear on how this equilibrium check should be carried out. Many algorithms are used next to each other. In this paper we adopted a systematic approach using the lower bound theorem of plasticity theory. According to this theorem every statically admissible equilibrium system gives a safe approximation of the strength. The algorithm selects the equilibrium system that provides the largest concrete stress f_{c1} .

In a crack the following stresses occur (Fig. 5.).

- f_{sxcr} normal stress in the reinforcing bars in the x -direction in a crack
- f_{sycr} normal stress in the reinforcing bars in the y -direction in a crack
- v_{ci} shear stress in a crack
- f_{ci} compression stress in a crack

The maximum value of the shear stress is (Walraven 1981)

$$v_{ci\max} = \frac{\sqrt{-f'_c}}{0.31 + 24w/(a + 16)} \quad (7)$$

where w is the crack width, a the diameter of the largest aggregate in mm and f'_c the compressive strength of the concrete in MPa. The compressive stress f_{ci} in a crack follows from the shear stress v_{ci} .

$$f_{ci} = \begin{cases} v_{ci\max} \left(1 - \sqrt{1.22(1 - |v_{ci}|/v_{ci\max})}\right) & \text{if } |v_{ci}| \geq 0.180 v_{ci\max} \\ 0 & \text{if } |v_{ci}| < 0.180 v_{ci\max} \end{cases} \quad (8)$$

The stresses in Figure 5 are averages over the surface of the panel. These are computed using the constitutive equations. The stresses in Figure 6 occur in a crack. The average stresses and stresses in the crack need to be in equilibrium. Two equilibrium equations can be formulated, for the x direction and the y direction.

$$\begin{aligned} f_{sxcr} \sin \theta \rho_x - v_{ci} \cos \theta - f_{ci} \sin \theta &= f_{sx} \sin \theta \rho_x + f_{c1} \sin \theta \\ f_{sycr} \cos \theta \rho_y + v_{ci} \sin \theta - f_{ci} \cos \theta &= f_{sy} \cos \theta \rho_y + f_{c1} \cos \theta \end{aligned} \quad (9)$$

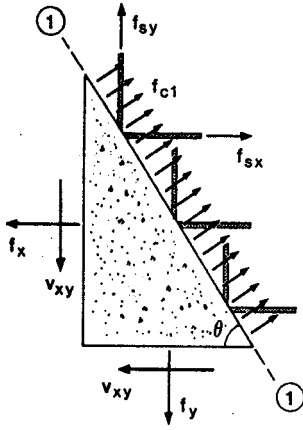


Figure 5. Average Stresses in a Section (Vecchio 1986)

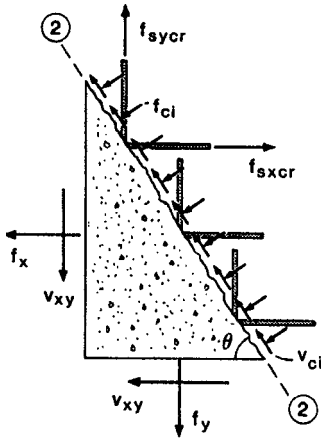


Figure 6. Stresses in a Crack (Vecchio 1986)

Equilibrium System 1

In equilibrium system 1, it is assumed that the reinforcement yields in both directions. Therefore $f_{sxcr} = f_{yx}$ and $f_{sycr} = f_{yy}$. The equilibrium

equations can be used to derive the shear stress v_{ci} in the crack and the average concrete stress f_{c1} .

$$\begin{aligned} v_{ci} &= (\rho_x(f_{yx} - f_{sx}) - \rho_y(f_{yy} - f_{sy})) \sin \theta \cos \theta \\ f_{c1} &= \rho_x(f_{yx} - f_{sx}) \sin^2 \theta + \rho_y(f_{yy} - f_{sy}) \cos^2 \theta - f_{ci} \end{aligned} \quad (10)$$

If the computed shear stress $|v_{ci}|$ is larger than the maximum shear stress $v_{ci\max}$ this equilibrium system cannot occur.

Equilibrium System 2

In equilibrium system 2, it is assumed that the reinforcing bars in the x direction yield and the crack starts to crush.

$$\begin{aligned} f_{sxcr} &= f_{yx} \\ v_{ci} &= v_{ci\max} \\ f_{sycr} &= \frac{1}{\rho_y} \left(\rho_x(f_{yx} - f_{sx}) - \frac{v_{ci\max}}{\sin \theta \cos \theta} \right) + f_{sy} \leq f_{yy} \\ f_{c1} &= \rho_x(f_{yx} - f_{sx}) - v_{ci\max} \left(\frac{1}{\tan \theta} + 1 \right) \end{aligned} \quad (11)$$

Equilibrium System 3

In equilibrium system 3, it is assumed that the reinforcing bars in the x direction yield and the crack starts to crush due to shear in the opposite direction as in equilibrium system 2.

$$\begin{aligned} f_{sxcr} &= f_{yx} \\ v_{ci} &= -v_{ci\max} \\ f_{sycr} &= \frac{1}{\rho_y} \left(\rho_x(f_{yx} - f_{sx}) + \frac{v_{ci\max}}{\sin \theta \cos \theta} \right) + f_{sy} \leq f_{yy} \\ f_{c1} &= \rho_x(f_{yx} - f_{sx}) + v_{ci\max} \left(\frac{1}{\tan \theta} - 1 \right) \end{aligned} \quad (12)$$

Equilibrium System 4

In equilibrium system 4, it is assumed that the reinforcement in the y direction yields and the crack starts to crush.

$$\begin{aligned} f_{sycr} &= f_{yy} \\ v_{ci} &= v_{ci\max} \\ f_{sxcr} &= \frac{1}{\rho_x} \left(\rho_y(f_{yy} - f_{sy}) + \frac{v_{ci\max}}{\sin \theta \cos \theta} \right) + f_{sx} \leq f_{yx} \\ f_{c1} &= \rho_y(f_{yy} - f_{sy}) + v_{ci\max} (\tan \theta - 1) \end{aligned} \quad (13)$$

Equilibrium System 5

In equilibrium system 5, it is assumed that the reinforcement in the y direction yields and the crack starts to crush due to shear in the opposite direction as equilibrium system 4.

$$\begin{aligned} f_{sycr} &= f_{yy} \\ v_{ci} &= -v_{ci\max} \end{aligned}$$

$$f_{sxc} = \frac{1}{\rho_x} \left(\rho_y (f_{yy} - f_{sy}) - \frac{v_{ci} \max}{\sin \theta \cos \theta} \right) + f_{sx} \leq f_{yx}$$

$$f_{cl} = \rho_y (f_{yy} - f_{sy}) - v_{ci} \max (\tan \theta + 1) \quad (14)$$

COMPUTATION OF CRACK WIDTHS

In case of a distributed crack pattern the crack spacing s_x for loading in the x direction only is (ENV 1992)

$$s_x = \frac{2}{3} \frac{d_x}{3.6 \rho_x} \quad (15)$$

where d_x is the bar diameter and ρ_x the reinforcement ratio. The crack spacing s_x for a loading in the y direction only is

$$s_y = \frac{2}{3} \frac{d_y}{3.6 \rho_y} \quad (16)$$

The crack spacing in the x and y direction have a maximum value of half the panel width and height. If the reinforcement ratio is smaller than the critical ratio than the crack distance is half the panel width. The crack spacing s perpendicular to the crack direction θ is

$$s = \frac{1}{\frac{|\sin \theta|}{s_x} + \frac{|\cos \theta|}{s_y}} \quad (17)$$

The crack width w is

$$w = s \varepsilon_1, \quad (18)$$

where ε_1 is the largest principle strain.

COMPUTATIONAL ALGORITHM

The constitutive model provides the stresses $\sigma_{xx}, \sigma_{yy}, \sigma_{xy}$ that result from the strains $\varepsilon_{xx}, \varepsilon_{yy}, \gamma_{xy}$. However, often engineers want to inverse this relation and compute the strains from imposed stresses. To this end the modified Newton-Raphson algorithm is very suitable.

$$\begin{bmatrix} \varepsilon_{xx} \\ \varepsilon_{yy} \\ \gamma_{xy} \end{bmatrix}_{\text{new}} = \begin{bmatrix} \varepsilon_{xx} \\ \varepsilon_{yy} \\ \gamma_{xy} \end{bmatrix}_{\text{old}} + K^{-1} \left(\begin{bmatrix} \sigma_{xx} \\ \sigma_{yy} \\ \sigma_{xy} \end{bmatrix}_{\text{imposed}} - \begin{bmatrix} \sigma_{xx} \\ \sigma_{yy} \\ \sigma_{xy} \end{bmatrix}_{\text{old}} \right) \quad (19)$$

For every iteration the inverse of the initial stiffness matrix K is used, which can be derived as

$$K^{-1} = \begin{bmatrix} \frac{1}{E_c + \rho_x E_s} & 0 & 0 \\ 0 & \frac{1}{E_c + \rho_y E_s} & 0 \\ 0 & 0 & \frac{2}{E_c} \end{bmatrix} \quad (20)$$

This algorithm proves to be very robust and sufficiently fast for real-time computations. The iterations start from zero strain and continue until sufficient convergence. The following termination criterion has been implemented.

$$\left\| \begin{bmatrix} \sigma_{xx} \\ \sigma_{yy} \\ \sigma_{xy} \end{bmatrix}_{\text{imposed}} - \begin{bmatrix} \sigma_{xx} \\ \sigma_{yy} \\ \sigma_{xy} \end{bmatrix}_{\text{new}} \right\| < 0.000001 \quad (21)$$

If 10000 iterations have occurred without satisfying the termination criterion the panel is assumed to have failed.

It was found that when a panel is loaded in two-way tension the algorithm computes perpendicular cracks that occur in the reinforcement directions (Fig. 7). However, due to an additional very small shear stress inclined cracks in only one direction occur. The inclination depends on the sign of the applied very small shear stress. Though experimental observations are not available, it is not probable that real panel behaviour would depend this strongly on a very small difference in loading. The conclusion is that the crack direction is not unique when a panel is loaded in two-way tension. The principal directions of the stresses and strains are either aligned or are very different.

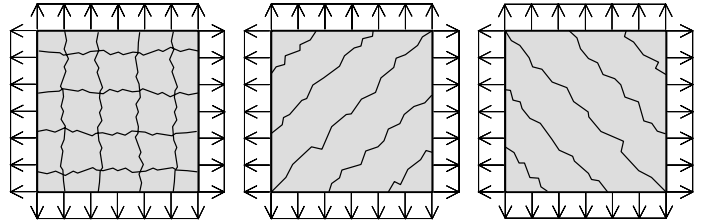


Figure 7. Possible crack solutions for a two-way tension loaded panel

The Newton-Raphson procedure finds the perpendicular crack solution when the starting strain values are $\varepsilon_{xx} = \varepsilon_{yy} = \gamma_{xy} = 0$. It finds either of the inclined crack solutions when the starting strain values are $\varepsilon_{xx} = \varepsilon_{yy} = 0, \gamma_{xy} = 0.0001$ or $\varepsilon_{xx} = \varepsilon_{yy} = 0, \gamma_{xy} = -0.0001$. The inclined solutions have the largest crack widths and therefore are most interesting for engineering design.

Alternatively, the Newton-Raphson procedure finds one of the inclined solutions when a small anomaly is introduced in the secant stiffness matrix.

$$K^{-1} = \begin{bmatrix} \frac{1}{E_c + \rho_x E_s} & 0 & 0 \\ 0 & \frac{1}{E_c + \rho_y E_s} & 0 \\ \frac{0.0001}{E_c} & 0 & \frac{2}{E_c} \end{bmatrix} \quad (22)$$

SIZE EFFECTS

Size effect in reinforced concrete is caused by the cracks. This is easily explained by the following thought experiment. Consider a concrete beam that is loaded and cracked. Suppose that a photo is made of this beam and that the photo is enlarged by a factor two compared to the original beam. The strains in the material of the enlarged photo will be the same as those in the original beam. The crack widths in the photo, however, will be twice as large. A wide crack has little aggregate interlock and little dowel action. Therefore, the stresses in the material of the photo would be the same but the stresses in the cracks of the photo would be smaller than the real beam. The stresses in the beam of the photo are not in equilibrium and need to redistribute. Consequently, the load platen of the photo carry less stress than the platen of the original beam.

Figure 8 shows ultimate load of a panel as a function of its size. All dimensions are factored by α . The panel size is $\alpha 600$ mm, the panel thickness is $\alpha 180$ mm, the bar diameters are $\alpha 15$ and $\alpha 16$ mm, the bar spacings are $\alpha 120$ and $\alpha 220$ mm of the x bars and y bars respectively. The aggregate size is $\alpha 30$ mm. The x bars are applied in 3 layers while the y bars are applied in 2 layers. The concrete compressive and tensile strength are -35.0 and 3.0 MPa respectively. Young's moduli of concrete and steel are 30000 and 210000 MPa respectively. The loading is factored by λ . The normal stresses are $\lambda 2.0$ and $\lambda 2.2$ MPa in the x and y direction respectively. The shear stress is $\lambda 4.75$ MPa. As Figure 8 shows a small size effect of 2.5% occurs.

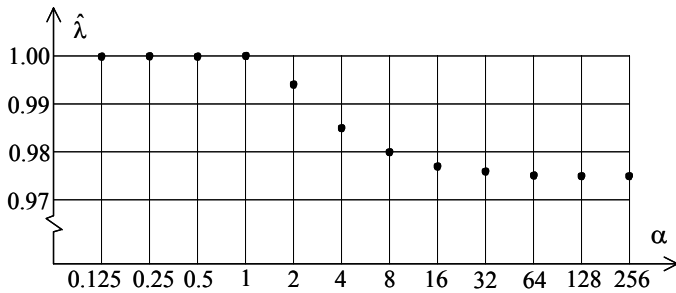


Figure 8. Ultimate load factor $\hat{\lambda}$ as a function of the size factor α

Figure 9. Shows the ultimate load as a function of the aggregate size only (*ceteris paribus*). The previous panel dimensions are adopted and $\alpha = 1$. A size effect of 7.5% occurs.

It can be shown that changes only in the height h of the previous panel do not change the ultimate loading (*ceteris paribus*). For small values of h the crack widths w are strongly reduced, up to 71%.

It can be concluded that the MCFT includes size effect because the stresses in the materials depend on the stresses in the cracks, which depend on the crack width, which in turn depends on the dimensions of a panel and reinforcing bars.

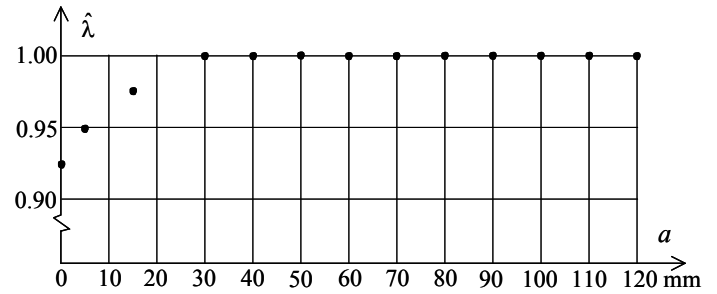


Figure 9. Ultimate load factor $\hat{\lambda}$ as a function of the aggregate size a

LOW REINFORCEMENT RATIOS

It was noticed that the MCFT is inaccurate for panels with low reinforcement ratios (Hoogenboom 2004). For example the MCFT predicts 38% more strength for panel PV2 of the experimental program of Vecchio (1986) (Table 1). This is probably caused by the high variability of the concrete tensile strength. A small specimen shows a substantially larger tensile strength because the chance on a weak spot is smaller than in a large panel (Weibull type size effect). However, the problem is alleviated because before any large loading occurs on a structure the concrete is already cracked due to shrinkage, drying and temperature changes.

The original MCFT first checks whether the average tensile stress is larger than the concrete tensile stress and subsequently the stress in the cracks is checked and reduced if necessary. In this paper it is proposed to check potential cracks already when the concrete is merely tensioned. Figure 10 shows the consequences for an uniaxial tensile test with a low reinforcement ratio. The left graph shows the result of the original MCFT and the right-hand graph shows the consequences of the proposed improvement.

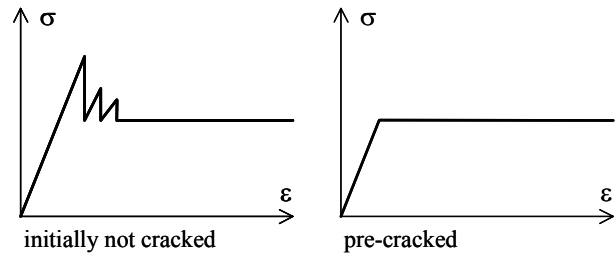


Figure 10. Stress-strain curves of reinforced concrete bars

Table 1 shows the experimental results of a number of panels with small reinforcement ratios. The panels are 70 mm thick and 890 mm wide in both directions. Young's moduli of the reinforcing bars are 210000 MPa. The bar diameters d_x , d_y and the bar spacings s_{bx} , s_{by} are included in the table. The bars form two nets in the panels. Columns 11 to 13 contain the loading ratios. Column 14 contains the experimental ultimate load factor. Column 15 and 16 contain the ultimate load factor according to the original MCFT and the MCFT including the proposed improvement respectively. The table shows that the proposed improvement has an effect on PV2 only. The original MCFT predicted 38% too much strength. Including the proposed improvement 34% too little strength is predicted. The latter is considered an improvement for two reasons; 1) it is a conservative prediction of the panel strength while the original MCFT overestimates the panel ultimate load strongly

and 2) in real structures less strength will be found than in laboratory conditions due to the pre-cracking that will occur in time.

The critical reinforcement ratio is defined as

$$\rho_{cr} = \frac{f_t}{f_y} \quad (23)$$

where f_t is the concrete tensile strength and f_y is the reinforcement yield strength. Panel PV2, PV13 and PV18 have reinforcement ratios less than the critical ratio in one or more directions (Table 2). In this situation just one crack can be expected in the panel. Despite an extensive search the authors did not find more experimental data on panels with a reinforcement ratio less than the critical ratio.

Size effects were not found in the strength of concrete panels with less than the critical reinforcement ratio. Despite an extensive parameter study it was not found using the original MCFT and not using the MCFT with the proposed improvement.

Table 2. Reinforcement ratios of the experiments

	ρ_x	ρ_y	ρ_{crx}	ρ_{cry}
PV2	<u>0.0018</u>	<u>0.0018</u>	0.0037	0.0037
PV3	0.0048	0.0048	0.0025	0.0025
PV13	0.0179	<u>0.0000</u>	0.0056	
PV16	0.0074	0.0074	0.0060	0.0060
PV17	0.0074	0.0074	0.0056	0.0056
PV18	0.0179	<u>0.0032</u>	0.0034	0.0035
PV19	0.0179	0.0071	0.0031	0.0048
PV20	0.0179	0.0089	0.0032	0.0049
PV29	0.0179	0.0089	0.0035	0.0048

CONCLUSIONS AND RECOMMENDATIONS

In analysis of reinforced concrete structures the material model should assume that the concrete is already cracked before the loading is applied. This prevents that unrealistic high strengths are found for structures with small reinforcement ratios. The assumed cracking

represents loading due to drying shrinkage and temperature changes which are almost always ignored in the structural analyses.

The modified compression field theory (MCFT) predicts a small size effect in the strength of some reinforced concrete panels loaded in plane stress. This size effect results from the behaviour of the cracks. Apparently, size effect can already be described by using an elementary material model as the MCFT. In the considered panels the predicted size effect is too small for experimental validation. More research is needed to determine whether the MCFT can predict size effects in reinforced concrete walls accurately.

If a panel is loaded in two-way tension the MCFT predicts that three different cracking solutions are possible. There are no experiments available that show which of the solutions is the correct one. For engineering design the solution with the largest crack widths are most interesting. The software finds this solution when a small anomaly is introduced in the stiffness matrix of the Newton-Raphson procedure.

There is a need for experiments on panels with less reinforcement than the critical ratio. Especially, data on crack widths is needed to validate commonly used material models for reinforced concrete.

REFERENCES

- ENV 1992 (1991). "Eurocode 2, Design of Concrete Structures, Part 1, General Rules and Rules for Buildings," European Prestandard, Brussels, CEN.
- Vecchio, FJ and Collins, MP (1986). "The Modified Compression Field Theory for Reinforced Concrete Elements Subjected to Shear," *ACI Structural Journal*, Vol 83 No 2, pp 219-231.
- Walraven, JC (1981). "Fundamental Analysis of Aggregate Interlock," *Proceedings ASCE*, Vol 107, ST11, pp 2245-2270.
- Hoogenboom, PCJ and Voskamp, W (2004), "Performance-Based Design of Reinforced Concrete Panels on the WWW", Proceedings of the 14th International Offshore and Polar Engineering Conference, *ISOPE 2004*, Toulon, France, May 23-28, 2004, pp. 276-282.

Table 1. Comparison of experimental and predicted strengths

	d_x mm	s_{bx} mm	d_y mm	s_{by} mm	f'_c MPa	f_t MPa	E_c MPa	f_{yx} MPa	f_{yy} MPa	σ_{xy}	σ_{xx}	σ_{yy}	Test MPa	MCFT MPa	MCFT+ MPa	MCFT+ / Test
PV2	2.1	55.0	2.1	55.0	-23.5	1.60	20400	428	428	1	0	0	1.16	1.60	0.77	0.66
PV3	2.1	20.6	2.1	20.6	-26.6	1.70	23100	662	662	1	0	0	3.07	2.94	2.94	0.96
PV13	4.5	25.4	0		-18.2	1.41	13500	248		1	0	0	2.01	1.41	1.41	0.70
PV16	2.1	13.4	2.1	13.4	-21.7	1.54	21700	255	255	1	0	0	4.12	1.88	1.88	0.46
PV17	2.1	13.4	2.1	13.4	-18.6	1.42	18600	255	255	0	-1	0	21.30	20.48	20.48	0.96
PV18	4.5	25.4	2.1	31.0	-19.5	1.46	17700	431	412	1	0	0	>3.04	2.98	2.98	0.98
PV19	4.5	25.4	2.1	13.9	-19.0	1.44	17300	458	299	1	0	0	3.95	3.80	3.80	1.09
PV20	4.5	25.4	2.1	11.1	-19.6	1.46	21800	460	297	1	0	0	4.26	4.30	4.30	1.01
PV29	4.5	25.4	2.1	11.1	-21.7	1.54	24100	441	324	1	-0.29	-0.29	5.87	6.58	6.58	1.12